

The superluminal motion of Gamma-Ray-Burst sources and the complex afterglow of GRB 030329

Shlomo Dado¹, Arnon Dar¹ and A. De Rújula^{1,2}

ABSTRACT

The source of the very bright Gamma-Ray Burst GRB 030329 is close enough to us for there to be a hope to measure or significantly constrain its putative superluminal motion. Such a phenomenon is expected in the “Cannonball” (CB) model of GRBs. Recent precise data on the optical and radio afterglow of this GRB—which demonstrated its very complex structure—allow us to pin down the CB-model’s prediction for the afterglow-source position as a function of time. It has been stated that (the unpublished part of) the new radio data “unequivocally disprove” the CB model. We show how greatly exaggerated that obituary announcement was, and how precise a refined analysis of the data would have to be, to be still of interest.

Subject headings: gamma rays: bursts

1. Introduction and summary

The currently best-studied theories of Gamma-Ray Bursts (GRBs) and their afterglows (AGs) are the *Fireball* models (see, e.g., Zhang & Meszaros 2003 for a recent review) and the *Cannonball* (CB) model (see, e.g., Dar & De Rújula 2003a; Dado, Dar & De Rújula, 2002a; 2003a and references therein). The first set of models is often considered to be *the standard model* of GRBs. In spite of their similarly-sounding names, these two models are (or were initially) completely different in their basic hypothesis, in their description of the data, and in their predictions. In this note we concentrate on a CB-model prediction which is not (to date) a standard-model one, the apparently superluminal motion of the source of GRBs and their afterglows: the “cannonballs”. In quite exceptional cases—relatively close-by GRBs with sufficiently bright (radio) AGs—it may be possible to observe this superluminal

¹dado@phep3.technion.ac.il, arnon@physics.technion.ac.il, dar@cern.ch.
Physics Department and Space Research Institute, Technion, Haifa 32000, Israel

²alvaro.derujula@cern.ch. Theory Division, CERN, CH-1211 Geneva 23, Switzerland

motion of CBs relative to “fixed stars”. Prior to GRB 030329, the case in which a possible superluminal motion (Dar & De Rújula 2000) came closest to being observable was that of GRB 980425, which could “almost” be classified (Dar & De Rújula 2003a) as an X-ray flash (XRF). For XRFs, the observation of a superluminal motion may be simpler than for GRBs, for the source’s apparent displacement in the sky is proportional to the (small) observer’s viewing angle, and we interpret XRFs as jetted GRBs viewed at larger angles (Dar & De Rújula 2003a; Dado, Dar & De Rújula 2003f). In a different model, this interpretation of XRFs has also been advocated by Yamazaki, Yonetoku & Nakamura (2003).

The CB-model is a very explicit elaboration of the original proposal by Shaviv and Dar (1995): that the γ -rays of a GRB would be generated by inverse Compton Scattering (ICS) of stellar light by the electron constituents of transient narrow jets, emitted in stellar processes leading to gravitational collapse.

In the CB model, long-duration GRBs, as well as XRFs (Dar & De Rújula 2003a; Dado, Dar & De Rújula 2003f) are produced in the explosions of *ordinary* core-collapse SNe, akin to SN1998bw³ (Dar & De Rújula 2000), the first SN to be observed in “association” with a GRB (GRB 980425, Galama et al. 1998). Two opposite jets of CBs are emitted in the process, travelling with initially large Lorentz factors: $\gamma_0 \sim 10^3$. The CBs initially expand (in their rest system) at a velocity comparable to, or smaller than, the speed of sound in a relativistic plasma ($c/\sqrt{3}$), so that the jet opening angle (subtended by a CB’s radius as observed from its emission point⁴) is $\alpha_j < 1/(\gamma_0 \sqrt{3})$. The CBs’ highly relativistic motion collimates their emitted radiation —the GRB and its AG— within a forward beam of characteristic opening angle $1/\gamma$. An observer sees the “Doppler-favoured” jet, travelling at a small angle $\theta = \mathcal{O}(1/\gamma)$ relative to the line of sight. Typically $\theta > \alpha_j$, so that the jet’s opening angle can be neglected and the observer’s angle is the *only* relevant one.

In the CB model, during the AG, the jet opening angle *diminishes* with time, while the beaming angle $1/\gamma(t)$ increases, both evolutions being due to the CB’s interaction with the matter of the interstellar medium (Dado, Dar & De Rújula, 2002a). As a consequence, the AG’s source becomes increasingly “pointlike”, and its motion in the sky can in principle be followed. Since a CB’s motion is relativistic for days or months of (observer’s) time, its

³The X-ray and radio signals of the SN1998bw/GRB980425 pair are, in the CB model, attributed and well fit to the CB’s AG, depriving the SN of these “peculiar” emissions. The observed large velocity of the SN’s ejecta is attributed to their being observed exceptionally close to the jet axis. Neither this SN, nor its GRB, were exceptional (Dar & Plaga 1999, Dar & De Rújula 2000, Dado et al. 2002a, 2003a).

⁴We are neglecting the initial CB’s radius, presumably comparable or not much bigger than that of the collapsed core of the parent star, and thus entirely negligible by the time the GRB is emitted.

apparent displacement in the sky is *superluminal* (Courdec 1939, Rees 1967), as we argued in Dar & De Rújula (2000).

The closest-by GRB observed so far —GRB 980425, at a redshift $z = 0.0085$ — came very close to having an observable superluminal motion (see Dado, Dar & De Rújula 2003a for a detailed discussion). In a GCN note (Dar & De Rújula 2003b) we argued that this motion may be observable in the next-closest GRB (030329, at $z = 0.1685$). In this note we sharpen the predictions for this putative motion, given the current availability of precise optical data at early times and times later than the first ~ 6 days (Lipkin et al. 2003 and references therein), as well as sparse X-ray data (Marshall & Swank 2003; Marshall, Markwardt & Swank 2003; Tiengo et al. 2003) and abundant radio data (Sheth et al. 2003; Berger et al. 2003; Pooley 2003; Kuno et al. 2004).

A very relevant new information (Lipkin et al. 2003 and references therein) on the AG of GRB 030329 is the abundance of multiple deviations of the optical light curves relative to a smoothly declining behaviour. We shall refer to these deviations as *features*. In Dado et al. (2003c) we attributed the most obvious optical-AG feature —a “shoulder” starting at $t \sim 1$ day (after burst)— to a transition between a first to a second dominant CB, a choice supported by the fact that the γ -ray light-curve of this GRB has a very clear two-pulse structure (Vanderspek et al. 2003; <http://space.mit.edu/Hete/Bursts/GRB030329/>; see also Vanderspek et al. 2004), as shown in Fig. (1). With the emergence of a handful of other similarly-significant features in the first week —fast ups and downs of the optical fluences, $F_\nu(t)$, by some 20 to 40%— a more elaborate interpretation is required. In the AG model $F_\nu(t)$ is a direct and *quasi-local* tracer of the density of the ISM through which a CB travels, a fact to which we have attributed previous similar observations, e.g. the “humps” in the optical AGs of GRBs 000301c and 970508 (Dado et al. 2002a). It is therefore necessary to investigate the effect of local ISM density-inhomogeneities on the expected superluminal motion. This is what we do in this note for the case of GRB 030329. We conclude that the sources’ motion results in a displacement of ~ 0.3 (0.6) mas from day 3 to day 30 (100) after burst. Detecting such a motion may not be out of the question.

For the benefit of readers not familiar with the CB model, we present in an appendix a brief overview of the model and its current confrontation with data. We also offer there some commentary on the evolution of the standard model.

2. The deceleration of a CB

The Lorentz factor $\gamma = \gamma(x)$ of a CB diminishes with the distance x from the parent SN, as its motion is decelerated by collisions with the constituents of the interstellar medium (ISM). In an approximately hydrogenic ISM of local number density $n_p(x)$, the evolution of $\gamma(x)$ is determined by energy-momentum conservation to be:

$$\frac{d\gamma}{\gamma^2} = -\frac{dx}{L(x)} \quad (1)$$

$$L(x) \equiv \frac{N_{CB}}{\pi R_\infty^2 n_p(x)}, \quad (2)$$

with N_{CB} the CB's baryon number and R_∞ its calculable asymptotic radius, reached within minutes of observer's time. For typical parameters, by the time $R(x) \approx R_\infty$, the function $\gamma(x)$ is still extremely well approximated by its initial value $\gamma_0 \equiv \gamma(0)$ (Dado et al. 2002a).

For an object travelling at nearly the speed of light the relation between dx and the element of observer's time, dt , is:

$$\frac{dx}{\gamma(x) \delta(x)} \simeq \frac{c dt}{1+z}, \quad (3)$$

where z is the cosmological redshift and $\delta(x)$ is the Doppler factor by which the energy of photons emitted by the CB is locally boosted by its relativistic motion. For the Lorentz factors and viewing angles relevant to our discussion, $\gamma^2 \gg 1$ and $\theta^2 \ll 1$, and

$$\delta = \frac{1}{\gamma(1 - \beta \cos \theta)} \approx \frac{2\gamma}{1 + \gamma^2 \theta^2}, \quad (4)$$

to an excellent approximation.

We may integrate Eqs. (1,2) to obtain:

$$\frac{1}{\gamma(x)} - \frac{1}{\gamma_0} = \int_0^x \frac{dx'}{L(x')}, \quad (5)$$

which, for any given $n_p(x)$, yields the explicit x -dependent Lorentz factor $\gamma(x)$. Substitute this result, with use of Eq. (4), into Eq. (3) and integrate:

$$t = \frac{1+z}{c} \int_0^x \frac{dx}{\gamma(x) \delta(x)}, \quad (6)$$

to obtain the explicit relation between observer's time t and travelled distance x . The last two equations are a parametric description of the function of actual interest, $\gamma(t)$.

For some simple density profiles the above formal exercise can be carried explicitly to the end. For a constant-density ISM, for instance, we may define:

$$L(x) = x_\infty \equiv \frac{N_B}{\pi R_\infty^2 n_p}, \quad (7)$$

and conclude that $\gamma(t)$ is the real root of the cubic:

$$\frac{1}{\gamma^3} - \frac{1}{\gamma_0^3} + 3\theta^2 \left[\frac{1}{\gamma} - \frac{1}{\gamma_0} \right] = \frac{2ct}{3(1+z)x_\infty}, \quad (8)$$

that is:

$$\begin{aligned} \gamma &= \gamma(\gamma_0, \theta, x_\infty; t) = B^{-1} [\theta^2 + C\theta^4 + 1/C], \\ C &\equiv \left[2 / \left(B^2 + 2\theta^6 + B\sqrt{B^2 + 4\theta^6} \right) \right]^{1/3}, \\ B &\equiv 1/\gamma_0^3 + 3\theta^2/\gamma_0 + 6ct/[(1+z)x_\infty], \end{aligned} \quad (9)$$

while the distance travelled by a CB at a given observer's time is:

$$x(t) = x_\infty \left[\frac{1}{\gamma(t)} - \frac{1}{\gamma_0} \right], \quad (10)$$

so that it takes a distance $x_{1/2} \equiv x_\infty/\gamma_0$ for the CB to half its original Lorentz factor. As we shall see in detail in the case of GRB 030329, by the time the distance $x_{1/2}$ is reached, the AG fluence, proportional to a high power of $\gamma(t)$, has decreased by more than one order of magnitude.

We have performed CB-model fits to the AG measurements of all the GRBs of known redshift, and found that the values of $x_{1/2}$ are spread over more than an order of magnitude, centering at ~ 100 pc (Dado et al 2002a). These are comparable to the radii of the *superbubbles* wherein most SN explosions take place, created by the stellar winds and explosions of many previous SNe in dense star-formation regions. The approximation of a constant density n_p , employed in the quoted fits, may be a fair first try for the density within the superbubble and in the galactic-halo regions close-to—but without—the superbubble. In the case of GRB 030329 we shall see that the density profile of the superbubble's surface, as traced by the CB's X-ray and optical fluences, is quite rich and interesting.

3. The superluminal motion of a CB

The transverse projected velocity in the sky of a CB relative to its parent SN can be obtained from Eq. (4):

$$V_{CB} = \sin\theta \frac{dx}{dt} \simeq \frac{\gamma\delta\theta}{(1+z)} c, \quad (11)$$

which, for typical parameters, is extremely superluminal. The resulting angular separation at time t is:

$$\Delta\alpha(t) = \frac{1}{D_A} \int_0^t V_{CB}(t') dt' \rightarrow \theta \frac{x_\infty}{D_A} \left[\frac{1}{\gamma(t)} - \frac{1}{\gamma_0} \right], \quad (12)$$

where $D_A = D_L/(1+z)^2$ is the angular distance to the SN/CB system and D_L is the luminosity distance (we use throughout a cosmology with $\Omega = 1$ and $\Omega_\Lambda = 0.7$). The last expression in the r.h.s. of Eq. (12) is valid for a constant-density ISM.

At late time, when $[\gamma(t)\theta]^2 \ll 1$, Eq. (4) implies that $\delta(t) \approx 2\gamma(t)$, while Eq. (9) implies that when $3[\gamma(t)\theta]^2 \ll 1$, $\gamma(t)$ approaches its asymptotic behaviour, $\gamma(t) \approx [2ct/3(1+z)x_\infty]^{-1/3}$. The corresponding asymptotic behaviour of $\Delta\alpha$ is, for a constant n_p :

$$\Delta\alpha(t) \sim \frac{\theta}{D_A} \left[\frac{2x_\infty^2 ct}{3(1+z)} \right]^{1/3}, \quad (13)$$

which, in practice, is a fair approximation for t larger than a few days. Since XRFs are GRBs seen at a relatively large θ , Eq. (13) implies that the superluminal motion in the former systems is relatively easier to observe. Moreover, the larger the value of θ , the smaller the values of D_A favoured by selection effects (detection thresholds). This also privileges XRFs over GRBs as potential targets for a search of a superluminal CB motion.

4. The afterglow of GRBs

In the CB model, the AGs of GRBs and XRFs consist of three contributions, from the CBs themselves, the concomitant SN, and the host galaxy:

$$F_{AG} = F_{CBs} + F_{SN} + F_{HG}. \quad (14)$$

The latter contribution is usually determined by late-time observations, when the CB and SN contributions become negligible, or from measurements with sufficient angular resolution to tell apart $F_{CBs} + F_{SN}$ from F_{HG} .

Let the unattenuated energy flux density of SN1998bw at redshift $z_{bw} = 0.0085$ (Galama et al. 1998) be $F_{bw}[\nu, t]$. For a similar SN placed at a redshift z (Dar 1999, Dar & De Rújula 2000, Dado et al. 2002a):

$$F_{SN}[\nu, t] = \frac{1+z}{1+z_{bw}} \frac{D_L^2(z_{bw})}{D_L^2(z)} A(\nu, z) F_{bw}[\nu', t'], \quad (15)$$

where $A(\nu, z)$ is the attenuation along the line of sight, $\nu' = \nu(1+z)/(1+z_{bw})$, and $t' = t(1+z_{bw})/(1+z)$. The simple ansatz that *all* long-duration GRBs would be associated

with SN1998bw-like SNe (Dar & Plaga 1999; Dar & De Rújula 2000; Dado et al. 2002a) has proven to be unexpectedly precise and successful. For the most precise test so far, that of the GRB 030329/SN2003dh pair, see, e.g., Dado et al. (2003c), Stanek et al. (2003), Matheson et al. (2003) and Hjorth et al. (2003).

The AG of the CBs is mainly due to synchrotron radiation from accelerated electrons in the CB’s chaotic magnetic field. At optical and higher frequencies, the AG has the approximate form (Dado et al. 2003a,c):

$$F_{CB}[\nu, t] \propto n_p^{(1+\hat{\alpha})/2} R_\infty^2 \gamma^{3\hat{\alpha}-1} \delta^{3+\hat{\alpha}} A(\nu, t) \nu^{-\hat{\alpha}}, \quad (16)$$

with $\hat{\alpha}$ changing from ~ 0.5 to ~ 1.1 as each given observed frequency exceeds the time-dependent “*injection bend*”:

$$\nu_b(t) \simeq 1.87 \times 10^3 [\gamma(t)]^3 \left[\frac{n_p}{10^{-3} \text{ cm}^3} \right]^{1/2} \text{ Hz}, \quad (17)$$

where n_p is the baryon density of the interstellar medium⁵. In the same approximation in which Eq. (13) was derived, the AGs of GRBs and XRFs have the asymptotic behaviour $F_\nu \sim \nu^{-1.1 \pm 0.1} t^{-2.13 \pm 0.1}$ (Dado et al. 2002a). At radio frequencies, the AG spectrum is affected by self-absorption in the CBs themselves, characterizable by a single parameter per CB: a “free-free” absorption frequency, ν_a (Dado et al. 2003a).

The attenuation $A(\nu, t)$ is a product of the attenuation in the host galaxy, in the intergalactic medium, and in our Galaxy. The attenuation in our galaxy in the direction of the GRB or XRF is usually estimated from the Galactic maps of selective extinction, $E(B - V)$, of Schlegel, Finkbeiner & Davis (1998), using the extinction functions of Cardelli et al. (1986). The extinction in the host galaxy and the intergalactic medium, $A(\nu, t)$ in Eq. (15), can be estimated from the difference between the observed spectral index *at very early time when the CBs are still near the SN* and that expected in the absence of extinction. Indeed, the CB model predicts —and the data confirm with precision— the gradual evolution of the effective optical spectral index towards the constant value ≈ -1.1 observed in all “late” AGs (Dado et al. 2002a; 2003a). The “late” index is independent of the attenuation in the host galaxy, since at $t > 1$ (observer’s) days after the explosion, the CBs are typically already moving in the low-column-density, optically-transparent halo of the host galaxy.

⁵In the CB model, the spectral evolution as $\hat{\alpha}$ changes from ~ 0.5 to ~ 1.1 , is interpolated by $(\nu/\nu_b(t))^{-0.5}/\sqrt{1 + [\nu/\nu_b(t)]^{1.1}}$ (Dado et al. 2003a).

5. Some lessons from past GRBs

The CB-model description of the R-band AGs of six representative GRBs of interest to the analysis of GRB 030329 are shown in Fig. (2), and discussed anon. In Dado et al. (2002a) we showed that, in the CB model, the AGs of the GRBs of known redshift measured at the time could be successfully explained by a single dominant CB launched in the explosion of a SN akin to SN1998bw and moving, after a couple of observer hours, in an approximately constant-density ISM. A typical example is that of GRB 990510. Two exceptions are GRB 990123 and GRB 021211, whose AGs were measured very early, at a time when their CBs may be piercing the expected $n_p \sim 1/r^2$ density profile generated by the pre-SN “wind” of the parent star. In the CB model, the early fluence of optical AGs is proportional to $n_e^{3/4} \approx n_p^{3/4} \propto r^{-3/2} \approx t^{-3/2}$, in excellent agreement with the observations (Dado et al. 2003b).

Prior to GRB 030329, there were three cases (GRBs 970508, 000301c and 021004) for which the data showed clear evidence for deviations from a smooth AG behaviour. In the case of GRB 000301c, we attributed the “residua” of the observational data relative to its smooth CB-model fit to moderate deviations of the ISM density (far from the parent SN) from a constant value. In the case of GRB 970508, we have actually fit the AG to a jump from one to another constant-density value (Dado et al. 2002a). For GRB 021004 we found it more natural to fit the AG to the contribution of two CBs, since in this case the γ -ray count-rate as a function of time has a very clear two-pulse (i.e. two-CB) structure (Dado et al. 2003d). Moreover, unlike for GRB 970508, our attempts to describe the AG of GRB 021004 in terms of density variations failed, while the two-CB description fits the general trend of the AG very well.

GRB 030329 also has a two-CB γ -ray structure, but an unprecedentedly non-smooth AG, presumably for the simple reason that the precision and continuity of the data are also unprecedented. In the case of this GRB, the question will arise whether or not we should interpret its peculiar AG shape to two CBs, to density fluctuations, or to a combination of both effects.

6. The afterglow of GRB 030329: the first two rounds

In Dado et al. (2003c) we made a “first-round” CB-model fit to the NIR-optical observations of the AG of this GRB, then extending up to day ~ 6 after burst. Since experience with all previously-measured AGs had given us confidence in the quality of the model, we extrapolated these fits to later times, and we predicted the presence of a SN akin to SN1998bw,

luminous enough to compete with the AG —and be discovered— ten days after burst⁶. SN2003dh was discovered 9.6 days after burst and turned out to be surprisingly similar to SN1998bw (Stanek et al. 2003; Matheson et al. 2003; Hjorth et al. 2003).

In a second round, we have now extended our original fit to include the X-ray data of RXTE (Marshall & Swank, 2003; Marshall, Markwardt & Swank, 2003) and XMM-Newton (Tiengo et al. 2003), as well as the radio data of Sheth et al. (2003) and Berger et al. (2003) and many more NIR-optical measurements (Lipkin et al. 2003 and references therein). The optical and X-ray data and the broad-band CB-model fit are shown in Fig. (3). The inclusion of the new data modifies the parameters of the original data-poor fit only at the 10% level, a satisfactory result. The photon-number light-curve of the γ rays of GRB 030329 consisted of two clear pulses, corresponding in the CB model to two dominant CBs, see Fig. (1). Consequently, the fit to the AG was again performed with the additive contribution of two separate CBs. In the optical domain, the two contributions correspond to the two shoulders, as illustrated in Fig. (4), wherein we show the R-band results and the separate contributions of the two CBs. The data variations relative to the predicted smooth AG light-curve, ups and downs of $\sim 1/2$ magnitude, are, as for GRBs 970508, 000301c (Dado et al. 2002a) and 021004 (Dado et al. 2003b), to be expected: they trace moderate deviations from a constant-density interstellar medium, as implied by Eqs. (16,17). These density variations are discussed in detail in the next section.

The radio data at different frequencies and their comparison with the CB-model fit are shown in Fig. (5). The fit to the data at $\nu = 4.86$ GHz is shown Fig. (6), wherein the contributions of the two CBs are separately shown. As for the optical data, Fig. (4), we conclude that the “late” ($t > 1$ d) radio data are also dominated by one of the CBs.

7. The afterglow of GRB 030329: third round

The rich structure of the AG of this GRB is shown in Fig. (7), in which Lipkin et al. (2003) have compared the R-band data to a “reference” (a double power-law of indices ~ -1 and ~ -2 , with the break at day ~ 5) by plotting the magnitude difference between the data and the reference. The CB-model description of the optical and radio AGs in Figs. (3) and (5) satisfactorily reproduces the observed general trends. But the description is unsatisfactory in that its residua are also significant, as we show in Fig. (8). These residua

⁶The fits discussed in the current paper would have given the same result, since from day ~ 6 they have also reached the predicted asymptotic behaviour $F_\nu \sim t^{-2.13}$, and in the CB model there is no need to hypothesize whether “breaks” in the AG fluence have occurred by a given time, there being no breaks.

are not unlike those in Fig. (7), but for the absence of a prominent “N” feature, which we view as the result of the comparison of a power law —unmotivated at early times— with the smoothly-varying data. The remaining features, particularly the more prominent ones occurring after $t \sim 1$ day, require an explanation.

The CB-model’s fluence of Eq. (16) is proportional to a power of the ISM’s electron density $n_e = n_p$ and, in that sense, it “traces” its local, instantaneous value. This tracing is not perfectly *local*, because F_{CB} depends on $\gamma(t)$, and this function reflects the integral effect of the ISM density that a CB has swept through its prior voyage. To reproduce the features still prominent in Fig. (8), we must assume a given non-trivial density profile and solve Eqs. (2) to (6) explicitly to obtain the function $\gamma(t)$ to be used as input in the expression for the fluence, Eq. (16). We have in the past done this for the AG of GRB 970508, as reproduced in Fig. (2).

The CBs of GRBs 970508 and 030329, as we shall see explicitly for the second one, are at a distance $x \sim 100$ pc from the SNe that emitted them, at an observer’s time $t \sim 1$ day. At a distance of that order, we expect the CBs to be exiting the superbubble where the SN explosion is very likely to have taken place. As they exit it, they may encounter successive density inhomogeneities produced by a succession of past SN explosions and stellar mass ejections, which created the bubble in the first place. We have considered the *structured density profile* shown (as a function of observer’s time) in Fig. (9), in which successive “onion peals” appear as abrupt density increases, followed by a decline proportional to $1/r^2$ (or, approximately, $1/t^2$), analogous to the closer-by profile of a “wind-fed” circumburst material. With such a profile of overdensities we obtain a description of the R-band AG whose residua (relative to the reference broken power-law introduced by the observers) are shown in Fig. (7) as the (red) line. The parameters of this fit are only slightly different from the ones for a constant $n_e \approx n_p$, but for a somewhat larger initial value of x_∞ for the CB dominating the AG at late times. The N feature is fairly well reproduced with the density profile of Fig. (9), which is constant up to day ~ 1.5 . The feature is, in this sense, a fake. The description of the later-time features, however, requires the structured density profile of Fig. (9).

Clearly the many-parameter exercise we just described is not a “fit”: it could easily be improved to obtain an even better description, and it is certainly not as “predictive” as our prior fits to the early part of the AGs of GRBs 990123 and 021211, from which we claimed to have successfully traced the magnitude and $1/r^2$ profile of the close-by circumburst density (Dado et al. 2003d). Yet, the description is phenomenologically satisfactory, in the sense that we can once again claim that, in the CB model, the shapes of AGs provide interesting and consistent *quasi-local* tracers of the ISM density through which the CBs travel. The

actual distance $x(t)$ from the SN at which the late-AG-dominating CB in GRB 030329 was, as seen at a given observer’s time t , is shown in Fig. (10), constructed with use of Eq. (6). Indeed, at the time at which the density inhomogeneities are apparent (t between ~ 1 and ~ 5 days) the CB is 100 to 200 pc away from the SN, a reasonable radius for the overdensities surrounding a superbubble.

Given the need to introduce density variations to describe the detailed behaviour of the AG, the question arises whether or not two CBs —as opposed to just one— are needed. Our attempts to describe the AG with just one CB and a variety of density profiles failed. The reason is simple and unavoidable: the density increase required to produce the AG’s “shoulder” at $t > 1$ day inescapably increases the rate at which $\gamma(t)$ decreases with time. This entails a fast fall-down of the fluence, following soon after the initial increase produced by the local density increase. The resulting light-curves rise and fall fast —like the one shown in Fig. (2) does in the case of GRB 970508— and they fail in the description of the AG of GRB 030329. Thus, two CBs appear to be necessary to understand the AG of GRB 030329, as they are for the description of its two-pulse GRB structure, shown in Fig. (1).

8. Density variations, as observed at different frequencies

We are primarily concerned in this note with the putative superluminal motion of the CBs of GRB 030329, and not with a complete description of its wide-band AG. Thus, we have limited our detailed analysis with a structured density profile to the R-band AG, as in Figs. (7), the complete broad-band analysis with density variations being very laborious.

The outcome of the discussion that follows is that the structure seen in the R-band AG should be *almost* achromatic for data ranging from X-ray to NIR frequencies, while the structures should progressively disappear at lower and lower radio frequencies. The X-ray and optical AGs are not perfectly achromatic because the injection-band frequency of Eq. (17) “crosses” a given frequency at different times. But the crossing of the optical frequencies typically occurs at $t \sim 1$ day and the light curves become increasingly achromatic thereafter. The radio AGs, on the other hand, are predicted to be strongly chromatic (Dado et al. 2003a). To be more specific, we quote from the mentioned reference:

“Electrons that enter a CB with an injection Lorentz factor $\gamma(t)$ are rapidly Fermi accelerated... On a longer time scale, they lose energy by synchrotron radiation, and their energy distribution evolves... Electrons with a large $\gamma \sim \mathcal{O}[\gamma(t)]$ emit synchrotron radiation, with no significant time-delay, at the observer’s optical and X-ray wavelengths. But the emission of radio is delayed by the time it takes the electrons to “descend” to an energy at

which their characteristic emission is in the observer’s radio band... Thus, the optical and X-ray AG emission starts ... a few observer’s seconds after the corresponding γ -ray pulse. The radio signal, on the other hand, must await a time Δt for the cumulated electrons to cool down.” Δt was explicitly estimated in Dado et al. (2003a) to be of $\mathcal{O}(1)$ day.

Applied to the case at hand of a varying ISM density, what this means is that the features observed in the optical AGs should be smoothed in the radio over intervals of $\mathcal{O}(1)$ day. These intervals are frequency-dependent: longer for the lower radio frequencies. The expected trend of features that progressively disappear as the frequency diminishes is precisely the trend observed in the radio data reproduced in Fig. (5). The “second-round” fit shown in the figure systematically overestimates the late results, also a consequence of having ignored the density enhancements.

9. The superluminal motion in GRB 030329

The location of the source of the AG of this GRB has been followed in detail by VLBA observers from day ~ 3 to day ~ 84 after burst (Taylor et al., to be published). The associated SN2003dh dominates the optical AG after day ~ 10 , but is negligible in the radio AG at all measured times. Thus, the location of the radio source(s) is the location of the CB(s), expected to be extremely superluminal in the CB model.

The values of the fit observer’s angles are very similar for the two CBs: $\theta[1] = 2.2$ mrad, $\theta[2] = 2.3$ mrad. The values of the initial Lorentz factors are not so different: $\gamma_0[1] = 1037$, $\gamma_0[2] = 1606$. But the values of the deceleration parameter are very different: $x_\infty[1] = 0.033$ Mpc, $x_\infty[2] = 0.37$ Mpc (these numbers refer to the initial x_∞ as in Eq. (7), still unaffected by the density variations occurring at $t > 1$ day). This is the main reason why the contribution of CB1 to the AG decays much faster with time than that of CB2, as implied by Eq. (8) and illustrated in Figs. (4,6). It is also the reason why the superluminal motion of CB1 is much slower than that of CB2, as implied by Eq. (12). We are therefore interested in the fastest-moving and late-AG-dominating cannonball: CB2.

In the absence of the density fluctuations of Fig. (9), the predicted angular displacement $\Delta\alpha(t)$ of CB2, as given by the integrated form of Eq. (12), would be that of the upper panel of Fig. (11). It is on the basis of our “first-round” constant-density fit that we predicted such a displacement in Dar & De Rújula (2003b). In the presence of the observed density fluctuations, the predicted $\Delta\alpha(t)$ is shown in the lower panel of Fig. (11), the result of the integration of the velocity V_{CB} in Eqs. (11,12), obtained from the full-fledged determination of $\gamma(t)$ from Eqs. (1) to (6). The density fluctuations are dominantly density enhancements,

implying a faster deceleration of the CB. Thus the significantly reduction in the predicted apparent superluminal motion. Alas, this prediction of the CB-model is, in the case of GRB 030329, harder to test than we originally thought.

10. Caveats?

In its current form, the theory of AGs in the CB model is based on an analogy with high-resolution observations of relativistic jets emitted by systems such as the microquasars SS 433 (<http://chandra.harvard.edu/photo/2002/0214/index.html>; http://chandra.harvard.edu/press/04_releases/press_010504.html), GRS 1915+105 (Mirabel & Rodriguez 1999; Dhawan et al. 2000) and XTE J1550-564 (Corbel et al. 2002); and active galactic nuclei, e.g. the quasar Pictor A, whose emitted CBs, as seen at X-ray wavelengths, seem to stop expanding laterally shortly after ejection, and to travel for hundreds of kpc, before they finally stop and blow up (Wilson, Young & Shopbell 2001; Grandi et al. 2003). The CB-model’s simple explanation for this surprising fact is the following (Dado et al. 2002a). The ambient protons intercepted by a CB in its voyage encounter its inner chaotic magnetic field and are reemitted roughly isotropically (in the CB’s rest system). This implies an inwards pressure that stops the CB’s expansion and that is asymptotically equal to the pressure of the CB’s inner magnetic field, which is thereby calculable. The corresponding deceleration law (at constant radius R_∞ and ISM density n_p) is that of Eq. (8).

The magnitude and time-dependence of the magnetic field determined as in the previous paragraph plays a crucial role in the prediction of the broad-band AG spectra, which in the CB model is extremely simple, parameter-thrifty, and successful (Dado et al. 2003a, 2003e), particularly in comparison with its standard counterpart (see, e.g. Granot & Sari 2002). In spite of their phenomenological success, our assumptions leading to calculable CB radii and magnetic fields are very bold, and are no doubt oversimplifications. To investigate their solidity, in Dado et al. (2002a) we also studied a different ansatz: that the CB’s radius R would keep on increasing constantly with dx , with the ISM density still kept approximately constant. This ansatz, which corresponds to a much faster CB deceleration than that of Eq. (8), failed miserably. But in between the two extremes (a non-increasing and a steadily increasing CB’s radius), it is clear that there should be choices of $R(x)$ and $n_p(x)$ that are phenomenologically satisfactory and yet, correspond to a *faster* CB deceleration than the simple one dictated by Eq. (8) at constant $R \times n_p$. For such choices the simplest predictions of superluminal velocities —that we have discussed— would result in overestimates. But it would be premature to modify the simple predictions of the CB model, which —so far— are successful.

11. Discussion

In the internal/external shock model of GRBs, the variability of AG light curves —the set of “features” that we have discussed— is attributed to patchy shells and refreshed shocks (see, e.g. Piran, Nakar & Granot 2003; Granot, Nakar & Piran 2003 and references therein). In the case of GRB 030329, the features are attributed to delayed collisions between late, relatively low- γ shells and the earlier higher- γ shells having decelerated in their interactions with the ISM. The timing and the Lorentz factors are chosen so that the early fast shells collide in a matter of (observer) seconds to produce the GRB peaks, while the slow shells catch up with the decelerated earlier ones at times of order days: some five order of magnitudes longer. The required amount of fine-tuning is considerable. The late shells bring in an energy injection an order of magnitude larger than that of the original blast wave. It would be interesting to know whether their collisions with the slowed-down shells are expected to give rise to GRB pulses as well, in which case GRBs should be “repeaters”.

In the CB model, as we have seen, all that is required to explain the AG “features” are ISM density inhomogeneities occurring at a natural distance from the parent SN: that corresponding to the radius of a superbubble. No new phenomena must be invoked and no GRB parameters must be fine-tuned with special care.

12. Conclusions

The data on GRB 030329 are now sufficiently complete to allow for a detailed prediction of the motion of the source of its AG —allegedly superluminal in the CB model. The γ -ray light-curve and the optical AG require the presence of two CBs, one of which dominates the AG at late times. The parameters needed to predict the motion of the two CBs in the sky are determined by the optical data, so that the individual motion of each CB is predicted. The main result of this paper is the prediction of the sky-motion of the fastest-moving CB, which dominates the late AG, and is shown in the lower panel of Fig. (11).

The main caveat concerning a putative superluminal signature (Dar & De Rújula 2000, 2003b) concerns the input to the estimate of its magnitude. Indeed, we have shown in this paper that the predictions are very sensitive to the details of the density profile of the ISM. But we are encouraged by the fact that in the only case in which the superluminal jets of CBs made by a core-collapse SN could be seen, they were seen. Indeed, observations of SN 1987A (Ninenson and Papaliolios, 1999) showed two sources, moving in opposite directions along the SN’s axis at (real) velocities compatible with the speed of light and at an apparent superluminal velocity for the approaching source. Mercifully, the jet of that SN was not

pointing in our direction (Dar, Laor & Shaviv 1998; Dar & De Rújula 2001b).

Regarding the search for a superluminal motion, we learned by reading the e-version of NYT 030529 (the New York Times of that date, in GRB’s parlance) that, according to Dale Frail “[*Our observations*] are sufficient to rule out predictions of the cannonball model”. We have shown that, indeed, the observations of complicated features in the optical AG of GRB 030329 imply that our earlier results (Dar & De Rújula 2003b) —which ignored the presence of these features— constituted an overestimate of the predicted superluminal displacement. In this sense, Frail was right in stating that the observations ruled out the *predictions*, as opposed to the model itself.

In a setting more scientific than the NYT, Bloom et al. (2003) state: “*Owing to the proximity and bright radio emission, high-resolution (~ 1 pc) Very Long Baseline Array imaging of the compact afterglow was used by Frail (2003) to **unequivocally disprove the cannonball model for the origin of GRBs.**” The emphasis is ours. We have seen that these news of the death of the CB model may have been premature. Even though Mark Twain eventually died for sure, the CB model —though probably not immortal— is still in an excellent shape. Yet, trying to disprove the best available model(s), or even the proof of a difficult theorem, is the acceptable standard attitude in many a realm of the exact sciences. In this sense, the apparently strong motivation of the quoted observers to disprove the CB model is —in our opinion, and regarding this particular model— the healthiest of all possible attitudes.*

Acknowledgements. One of us (A. De R.) is indebted to the Physics Department and Space Research Institute of Technion for its hospitality. This research was supported in part by the Helen Asher Space Research Fund for research at the Technion.

13. Appendix: The CB model

In this model, the *engines* generating long-duration GRBs and XRFs are ordinary core-collapse SNe. Following the collapse of the stellar core into a neutron star or a black hole, and given the characteristically large specific angular momentum of stars, an accretion disk or torus is hypothesized to be produced around the newly-formed compact object, either by stellar material originally close to the surface of the imploding core and left behind by the explosion-generating outgoing shock, or by more distant stellar matter falling back after its passage (De Rújula 1987). A CB is emitted, as observed in microquasars, when part of the accretion disk falls abruptly onto the compact object (e.g. Mirabel & Rodriguez 1999; Rodriguez & Mirabel 1999 and references therein). The CBs of a GRB are assumed to me

made of ordinary hydrogenic matter. This is also in analogy to microquasar CBs, observed to be made of ordinary matter, as opposed to the standard-model contrived mixture of baryons and e^+e^- pairs. Indeed, blueshifted and redshifted H, He, metal and heavy-element optical and UV lines were detected from the approaching and receding CBs emitted by the microquasar SS433; see, e.g. Eikenberry et al. (2001), Gies et al. (2002).

In the CB model, SN1998bw, associated with GRB 980425, is an ordinary core-collapse SN (Dar and Plaga 1999; Dar and De Rújula 2000): its “peculiar” X-ray and radio emissions were not emitted by the SN, but were part of the GRB’s AG (Dado et al. 2002a, 2003a). The GRB appeared to be underluminous because it was viewed further off axis than others⁷ (e.g., Dar and De Rújula 2000). Thus, it makes sense in this model to expect an association between (long) GRBs and SN1998bw-like engines, transported to the GRB location (Dar 1999). The a-posteriori analysis of Dado et al. (2002a) of all the available data supported the conclusion that *all* (long) GRBs are indeed associated with such SNe⁸. In several more recent cases we used the CB model to *predict* how the associated SN would compare with the rest of the AG (GRB 011121, 020405, 021211; Dado et al. 2002b, 2002c, 2003d). The most interesting case is that of GRB 030329/SN2003dh, for which we also foretold the date when the SN would be dominant enough to be discovered (Dado et al. 2003c).

The fraction of visible GRBs, relative to the SNe that produce them, is $f \sim 2 \theta_{max}^2 / (4 \pi)$, where θ_{max} is some effective value of the maximum observer’s angle for which GRBs have been detectable. In practice θ_{max} is a few milliradians (Dado, Dar & De Rújula 2002a). This brings the *total* rate of (observed or unobserved) GRBs to a value close to that of core collapse SNe. This implies that a good fraction of such SNe may produce long-duration GRBs⁹ (Dar & Plaga 1999; Dar & De Rújula 2000).

13.1. The GRBs and XRFs themselves

In Dar & De Rújula (2000) the initial Lorentz factor of the CBs was argued to be $\gamma_0 \sim 10^3$, a choice corroborated by all our subsequent analyses. The high-energy photons of a single pulse in a GRB or an XRF are produced as a CB coasts through the “ambient light”

⁷This conclusion has been recently “standardized” (i.e. incorporated into standard GRB models without proper reference) by Granot, Panaitescu, Kumar & Woosley (2002).

⁸With use of an unmotivated “break-time” model of AGs, Zeh, Klose and Hartmann (2003) have recently reached and standardized this old conclusion of ours.

⁹A conclusion recently standardized by Lamb, Donaghy & Graziani (2003).

permeating the surroundings of the parent SN. The electrons enclosed in the CB Compton up-scatter photons¹⁰ to energies that, close to the CBs’ direction of motion, correspond to the γ -rays of a GRB and less close to it, to the X-rays of an XRF¹¹. Each pulse of a GRB or an XRF corresponds to one CB. The timing sequence of emission of the successive individual pulses (or CBs) reflects the chaotic accretion process and its properties are not predictable, but those of the single pulses are (Dar & De Rújula 2003a and references therein). In practice GRBs are observable for $\theta = \mathcal{O}(1/\gamma_0)$, XRFs are the same phenomenon, observed from somewhat larger angles (Dar & De Rújula 2003a; Dado, Dar & De Rújula 2003f).

GRBs are notorious for their variety. Yet, they have some two dozen common properties. The characteristic γ -ray energy is surprisingly narrowly distributed around $E = 250$ keV. The energy spectra are well fit by a specific “Band” function. The total “equivalent spherical energies” are distributed over a wide range, that becomes very narrow for the “true” (beaming-corrected) energy values. The photons arrive in successive pulses with fairly similar time-profiles which, in “long” GRBs, have a median width of 0.5 seconds. The γ -ray polarization is nearly maximal. A long list of phenomenologically-observed correlations between many different GRB observables appear to be well satisfied. *All* of these properties are very simply and successfully explained by the CB model, in a manner that does not require the introduction of *any* ad-hoc parameters (Dar & De Rújula 2003a and references therein).

13.2. GRB (and XRF) afterglows

In the AG phase, and within a few observer minutes from the end of a GRB’s intense γ emission, the emissivity of a CB is dominated by synchrotron emission from the electrons that penetrate in it as it propagates in the ISM. Integrated over frequency, this synchrotron emissivity is proportional to the energy-deposition rate of the ISM electrons in the CB. These electrons are “Fermi-accelerated” in the CB’s tangled magnetic maze to a broken power-law energy distribution with a “bend” energy equal to their incident energy in the CBs’ rest frame, $E = \gamma(t) m_e c^2$. Their synchrotron radiation—the afterglow—is collimated and Doppler-boosted by the relativistic motion of the CBs. The radiation is also redshifted by the cosmological expansion and attenuated on its way to an earthly observer, during its

¹⁰Inverse Compton scattering by narrow jets was proposed as *the mechanism* for GRB generation by Dar & Shaviv (1995). Much later, it was attributed in a first electronic version of Lazzati et al. (2003) to Lazzati et al. (2000), an attribution subsequently retracted (Lazzati et al. 2000, second version). More recently and apparently unaffected, Lazzati (2003) attributes the mechanism once again to Lazzati et al. (2000).

¹¹This conclusion has been enthusiastically standardized by Donaghy, Lamb, Graziani (2003) and Lamb, Donaghy & Graziani (2003a,b,c). Their model requires parent stars that span faster in the distant past.

passage through the CB itself, the host galaxy, the intergalactic space and our own galaxy.

The approximate CB-model analysis of the fluences of GRB AGs, as functions of time and frequency, is fairly simple. Besides z and θ (which are not parameters specific to the model) it involves only three quantities: γ_0 , x_∞ , an overall normalization, and ν_a (a *single* free-parameter frequency pertinent to the radio-absorption within a CB). In spite of its economy of parameters (notorious in the case of the wide-band spectral shapes) the CB model satisfactorily describes—in a unified manner—all measured GRB AGs, including that of GRB 980425 (e.g., Dado et al. 2002a, 2003a, 2003e). Our impression is that no such claims can be made in the realm of standard GRB models.

REFERENCES

- Berger, E., et al. 2003, Nature, 426, 154
- Blake, C. & Bloom, J. S. 2003, GCN Circ. 2011
- Bloom, J. S., et al. 2003, astro-ph/0308034
- Cardelli, J. A., Clayton, G. C. & Mathis, J. S. 1989, ApJ, 345, 245
- Corbel, S., et al. 2002, Science, 298, 196
- Courdec, P. 1939, Annales d’Astrophysique 2, 271
- Dado, S., Dar A. & De Rújula, A. 2002a, A&A, 388, 1079
- Dado, S., Dar A. & De Rújula A. 2002b, ApJ, 572, L143
- Dado, S., Dar A. & De Rújula A. 2002c, A&A, 393, L25
- Dado, S., Dar A. & De Rújula A. 2003a, A&A, 401, 243
- Dado, S., Dar A. & De Rújula A. 2003b, ApJ, 585, L15
- Dado, S., Dar A. & De Rújula A. 2003c, ApJ, 594, L89
- Dado, S., Dar A. & De Rújula A. 2003d, ApJ, 593, 961
- Dado, S., Dar A. & De Rújula A. 2003e, Phys. Lett. B562, 161
- Dado S., Dar A. & De Rújula A. 2003f, astro-ph/0309294
- Dahawan, V., Mirabel, F. & Rodriguez, L. F. 2000, ApJ, 543, 373

- Dar, A. & De Rújula, A. 2000, astro-ph/0008474
- Dar, A. & De Rújula, A. 2001, in *Astrophysics and Gamma Ray Physics in Space*; eds. A. Morselli and P. Picozza; Frascati Physics Series Vol. XXIV (2002), pp. 513-523; astro-ph/0110162
- Dar, A. & De Rújula, A. 2003a, astro-ph/0308248
- Dar, A. & De Rújula, A. 2003b, GCN Circ No. 2133
- Dar, A., Laor, A. & Shaviv, N. J. 1998, Phys. Rev. Lett. 80, 5813
- Dar, A., & Plaga, R. 1999, A&A, 349, 259
- Dar, A. 1999, A&AS, 138, 505
- Dar, A. 2003, astro-ph/0301389
- De Rújula, A. 1987, Phys. Lett. 193, 514
- De Rújula, A. 2002, astro-ph/0207033
- Donaghy, T. Q., Lamb, D. Q. & Graziani, C. 2003, astro-ph/031496
- Eikenberry, S. S., et al. 2001, ApJ, 561, 1027
- Esin, A. A. & Blandford, R. 2000, ApJ, 534, L151
- Frail, D. A., et al., 2001, ApJ, 562, L55
- Frail, D. A. 2003, American Astronomical Society Meeting, 2003
- Frederiksen, J. T., Hedelal, C. B., Haugbolle, T. & Nordlund, A. astro-ph/0303360
- Galama, T. J., et al. 1998, Nature 395, 670
- Ghisellini, G. & Lazzati, D. 1999, astro-ph/9906471
- Gies, D. R., et al. 2002, ApJ, 566, 1069
- Grandi, P., et al. 2003, 2003, ApJ, 586, 123
- Granot, J., Nakar, E., Piran, T. 2003, Nature 426, 138
- Granot, J. & Sari, R. 2002, ApJ. 568, 820
- Granot, J., Panaitescu, A., Kumar, P. & Woosley, S. E. 2002, ApJ, 570, L61

- Greiner, J., et al. 2003a, GCN Circ. 2020
- Greiner, J., et al. 2003b, astro-ph/0311282
- Hjorth, J., et al. Nature 2003, 423, 847
- Hurley, K., Sari, R. & Djorgovski, S. G. 2002, astro-ph/0211620
- Henden, A. A., et al. 2003, GCN Circ. 2082
- Kuno, N., et al. 2004, astro-ph/0401258
- Lamb, D. Q., Donaghy, T. Q. & Graziani, C. 2003a, astro-ph/0309456
- Lamb, D. Q., Donaghy, T. Q. & Graziani, C. 2003b, astro-ph/0309463
- Lamb, D. Q., Donaghy, T. Q. & Graziani, C. 2003c, astro-ph/030504
- Lazzati, D., Rossi, E., Ghisellini, G. & Rees, M. 2003, astro-ph/0309038,
- Lazzati, D., Ghisellini, G., Celotti, A. & Rees, M. 2000, ApJ, 529, L17
- Lazzati, D. 2003, astro-ph/0312331
- Li, W., Filippenko, A.V., Chornock, R. & Jha, S. 2003, ApJ, 586, L9
- Lipkin, H. Y., et al. 2003, astro-ph/0312594
- Margon, B. A. 1984, ARA&A, 22, 507
- Marshall, F. E. & Swank, J. H. 2003, GCN Circ. 1996
- Marshall, F. E., Markwardt, C. & Swank, J. H. 2003, GCN Circ. 2052
- Matheson, T., et al. ApJ, 2003, 599, 394
- Meszáros, P. & Rees, M. J. 1999, MNRAS, 306, L39
- Mirabel, F. & Rodríguez, L. F. 1999, ARA&A, 37, 409
- Nisenson, P. & Papaliolios, C. 1999, ApJ, 518, L29
- Patat, F., et al. 2001, ApJ, 555, 900
- Peterson, B. A. & Price, P. A. 2003, GCN Circ. 1985
- Piran, T., Nakar, E. & Granot, J. 2003, astro-ph/0312138

- Pooley, G. 2003, GCN Circs. 2043, 2072
- Ramirez-Ruiz, E., Dray, L. M., Madau, P. & Tout, C. A. 2001, MNRAS, 327, 829
- Rees, M. J. 1967, MNRAS, 135, 345
- Rees, M. J. & Meszaros, P. 1992, MNRAS, 258, L41
- Reichart, D. E., 2001, ApJ, 554, 643
- Rodriguez, L. F. & Mirabel, I. F. 1999, ApJ, 511, 398
- Rykoff, E. S., et al. 2003, GCN Circ. 1995
- Sari, R. & Piran, T. 1999, A&AS, 138, 537
- Sari, R. 1999, ApJ, 524, L43
- Shaviv, N. J. & Dar, A. 1995, ApJ, 447, 863
- Sheth, K., et al. 2003, ApJ, 595, L33
- Schlegel, D. J., Finkbeiner D. P. & Davis M. 1998, ApJ, 500, 525
- Stanek, K. Z., et al. 2003, ApJ, 591L, 17
- Tiengo, A., Mereghetti, S., Ghisellini, G., Rossi, E., Ghirlanda, G. & Schartel, N. 2003, astro-ph/0305564
- Torii, K. 2003, GCN Circ. 1986
- Vanderspek, V., et al. 2003, GCN Circ. 1997
- Vanderspeck, R., et al. 2004, astro-ph/0401311
- Waxman, E. 2003, astro-ph/030351
- Waxman, E. & Draine, B. T. 2000, ApJ, 537, 796
- Wilson, A. S., Young, A. J. & Shopbell, P. L. 2001, ApJ, 547, 740
- Yamazaki, R., Yonetoku, D. & Nakamura, T. ApJ, 2003, 594, L79
- Zeh, A., Klose, S. & Hartmann, D. H. astro-ph/0311610
- Zhang, B. & Meszaros, P. 2003, astro-ph/0311321

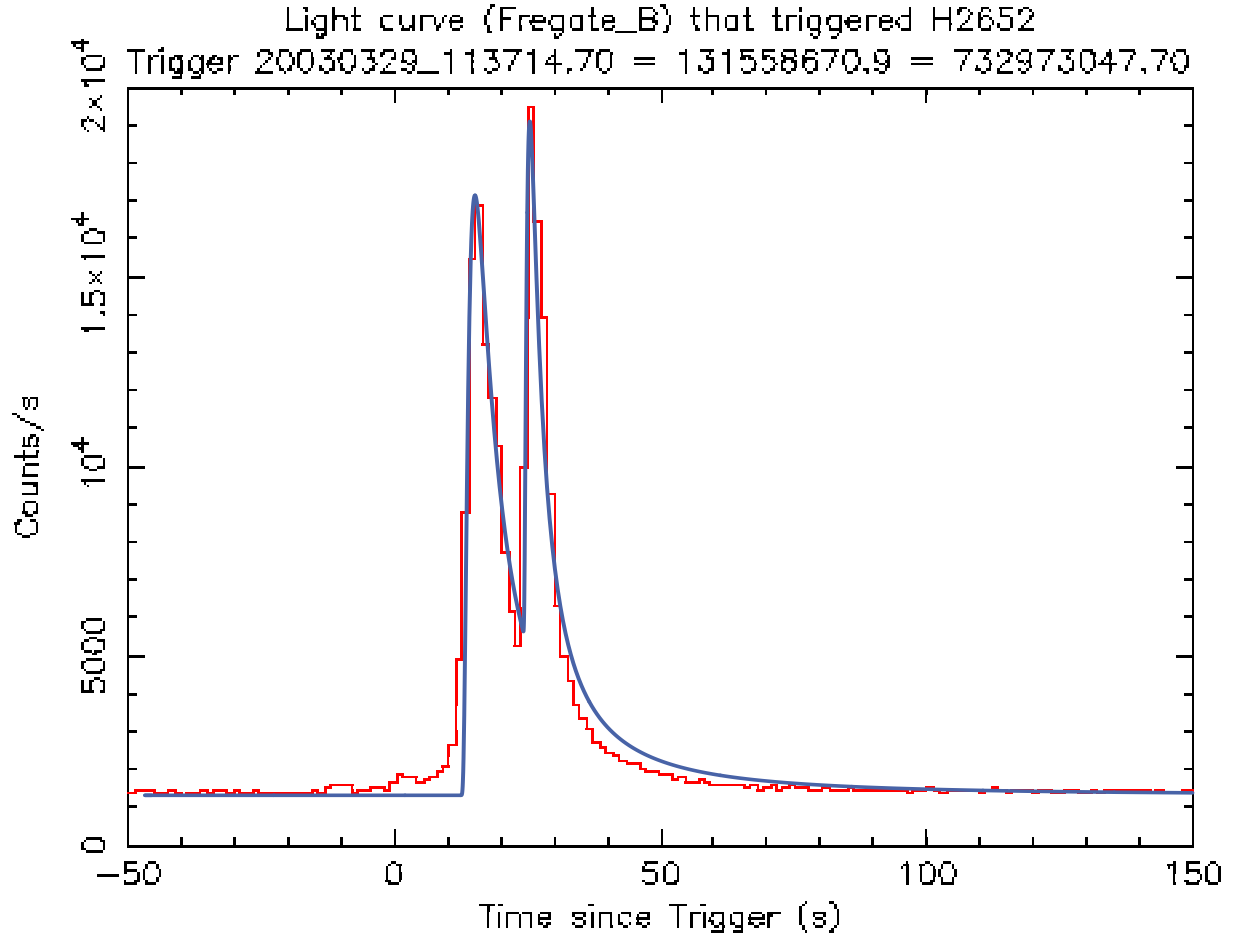


Fig. 1.— The γ -ray light curve of GRB 030329, the (red) binned curve (Vanderspeck et al. 2004); and its simplest CB-model description, the (blue) continuous line (Dado et al. 2003c).

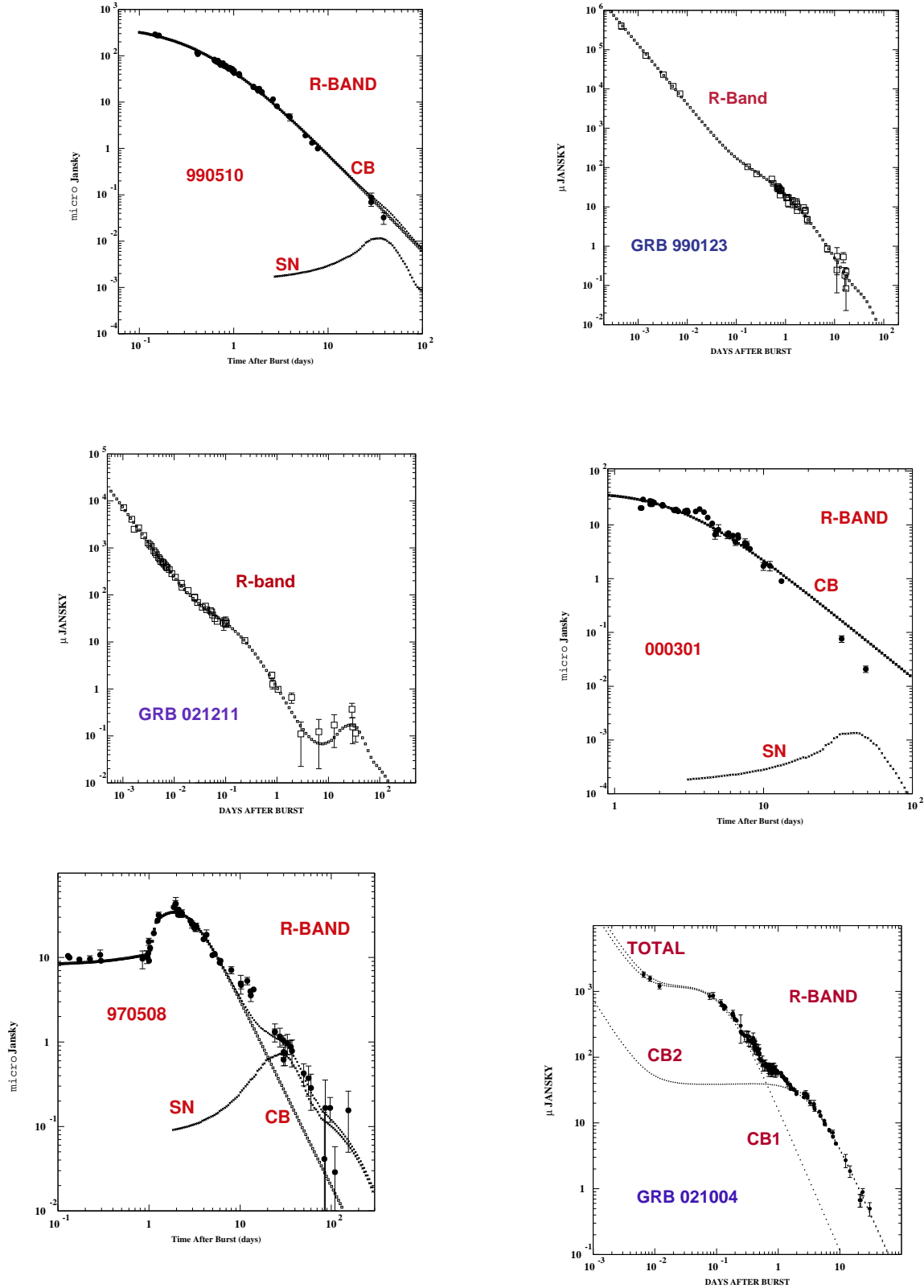


Fig. 2.— R-band AGs of six representative GRBs of interest to the analysis of GRB 030329, and their CB-model fits. In a CB-model analysis, there is evidence for a SN akin to SN1998bw (transported to the GRB location) in the AG of all GRBs in which such a contribution is discernible (in practice all GRBs with $z < 1.1$).

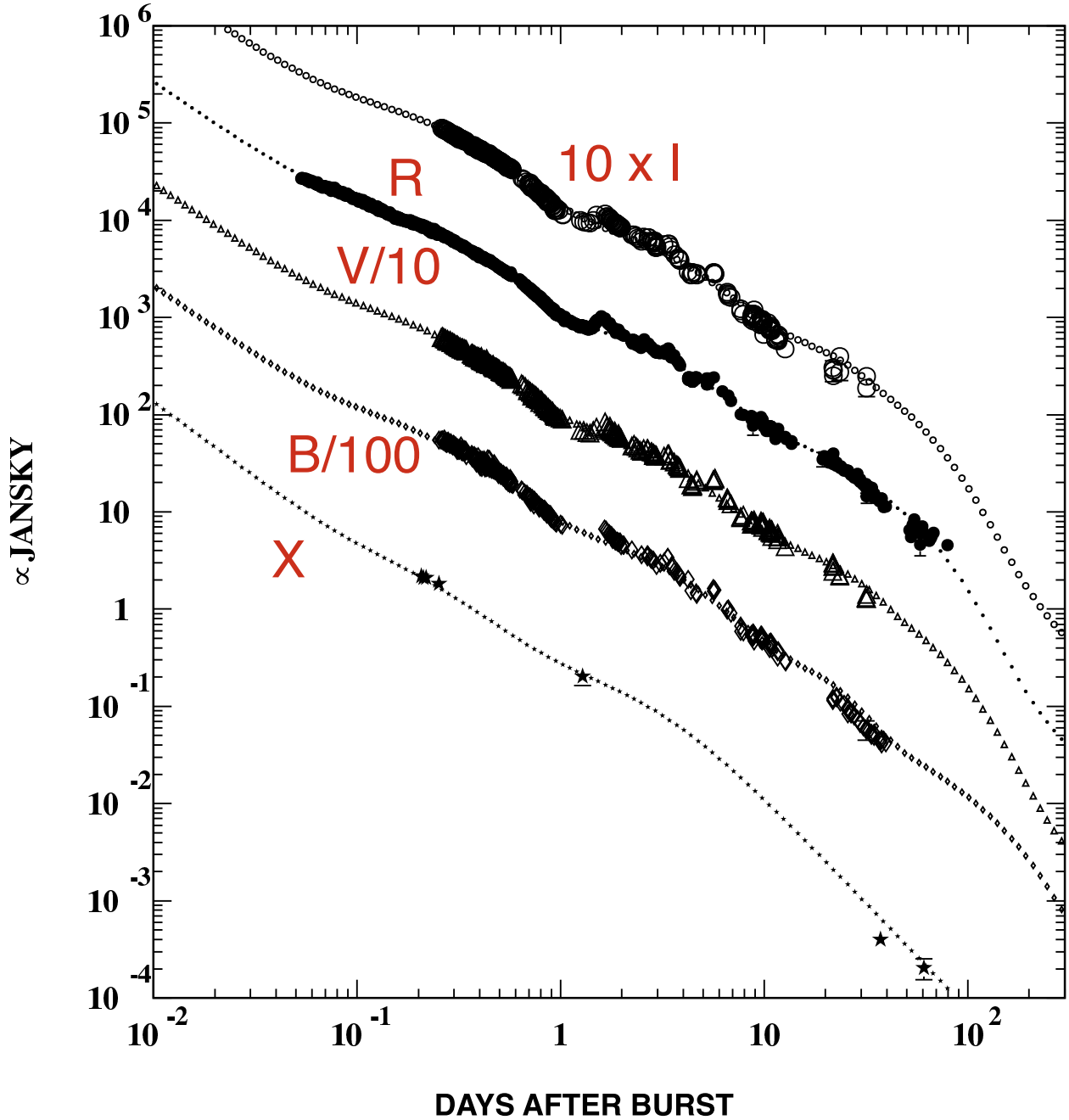


Fig. 3.— The NIR–optical and X-ray observations of the AG of GRB 030329 and the “second-round” broad-band fit for two CBs with different parameters, described in the text. The ISM density is assumed to be a constant plus a “wind” contribution decreasing as $1/r^2$. The various bands are scaled for presentation. The fit is to the X-ray data of RXTE (Marshall & Swank, 2003; Marshall, Markwardt & Swank, 2003) and XMM-Newton (Tiengo et al. 2003) and many other NIR–optical measurements, recalibrated by Lipkin et al. (2003 and references therein); as well as the radio data of Sheth et al. (2003) and Berger et al. (2003), which are shown in Fig. (5). The host-galaxy’s contribution was neglected. The individual bands have been rescaled for clarity.

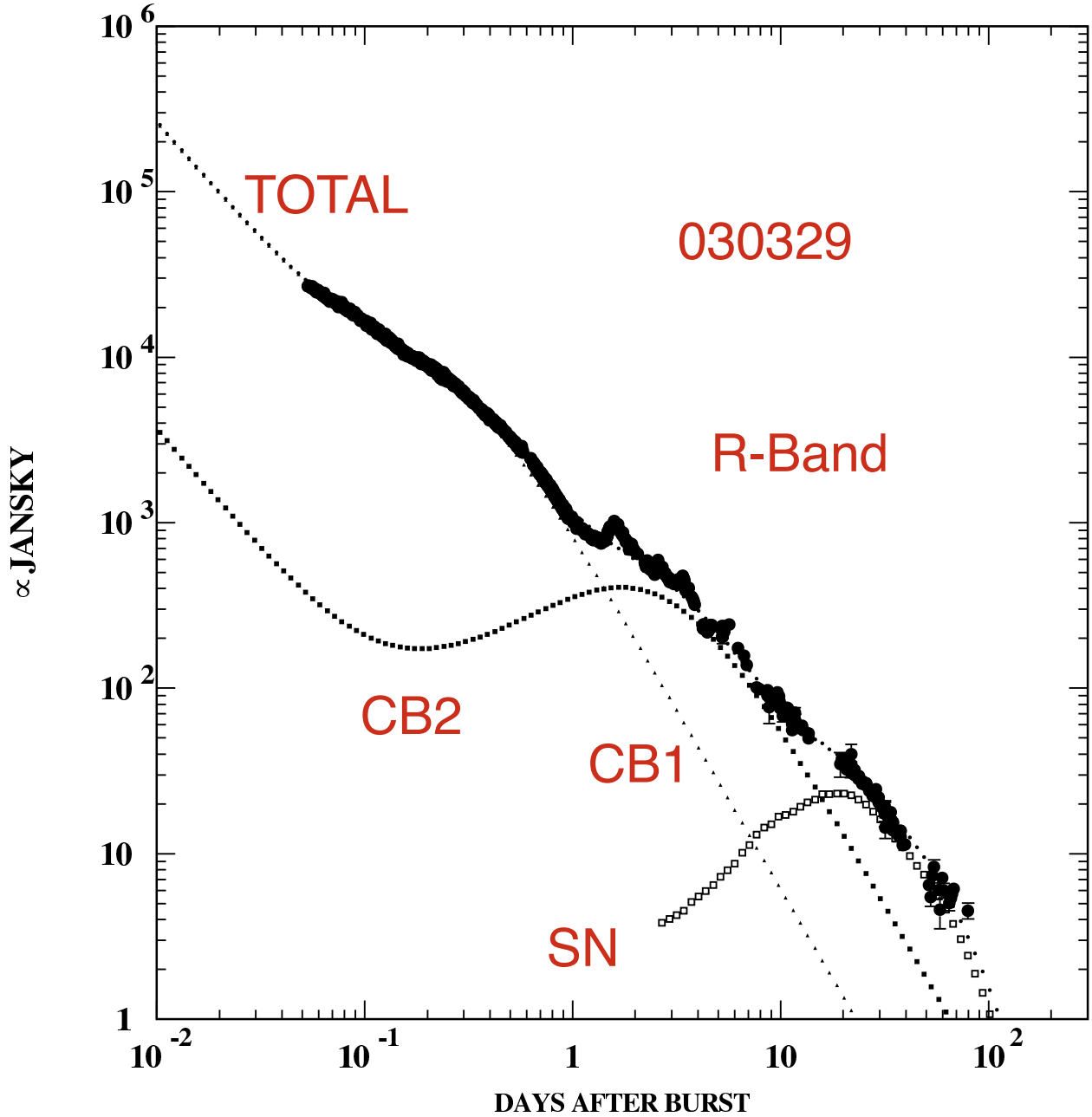


Fig. 4.— Blow-up of the R-band results of Fig. (3). The ISM density was assumed to be a constant plus an additional “wind” contribution decreasing as $1/r^2$. The wind contribution is only significant at $t < 0.1$ days, after which the CBs are more than 10 pc away from the progenitor. This “wind” contribution is also seen in other AGs observed early enough, e.g. GRBs 990123, 021211 and 021004, shown in Fig. (2). The individual contributions of the two CBs and of a SN akin to SN1998bw (at the GRB’s redshift) are also shown; the cannonball “CB2” dominates the AG at late times. We attribute the “residua” of this “second-round” fit to having ignored the ISM density inhomogeneities at $t > 1$ day, as explained in the text. A fit with two distinct CB contributions was previously needed for the description of GRB 021004, shown in Fig. (2), which also had a double-peak (two-CB) γ -ray light curve.

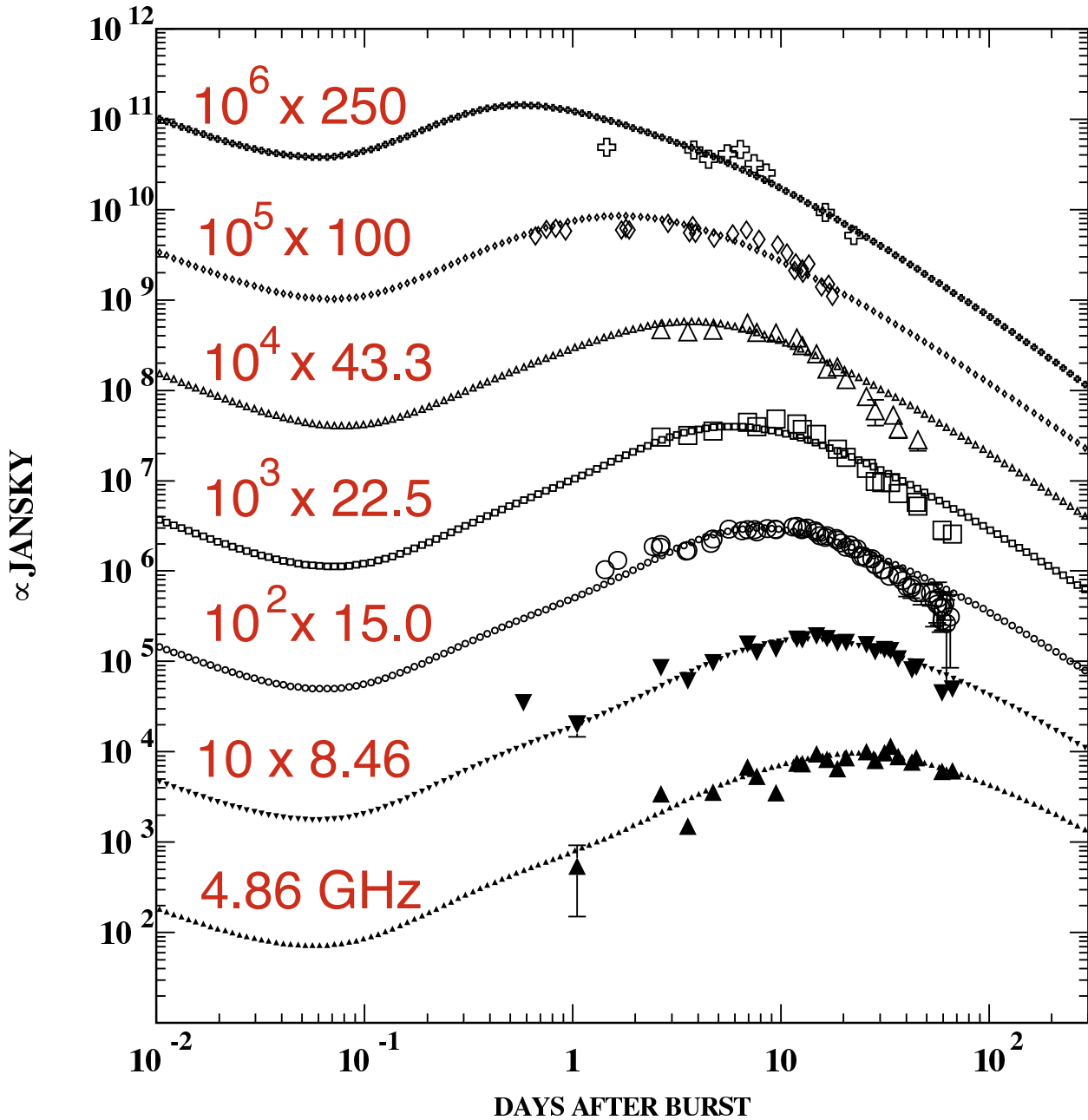


Fig. 5.— The radio observations, ranging from 4.86 to 250 GHz, of the AG of GRB 030329 (Sheth et al. 2003 and Berger et al. 2003) and the CB-model “second-round” broad-band fit with two CBs to these data and the ones shown in Fig. (3). The various frequencies have been scaled for presentation. We attribute the “residua” of this fit to having ignored the ISM density inhomogeneities at $t > 1$ day, as explained in the text.

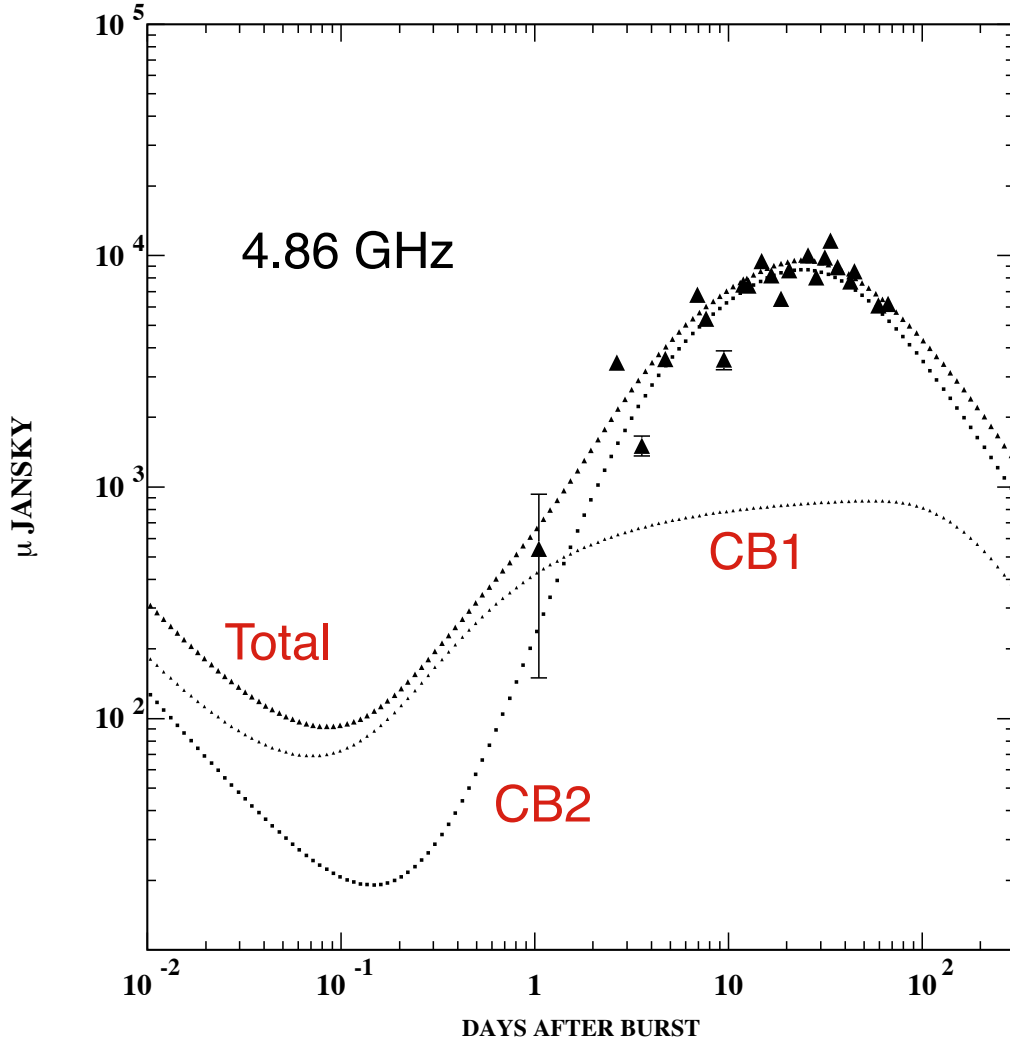


Fig. 6.— Blow-up of the 4.86 GHz results of Fig. (5). The best fit with two CBs is shown, as well as their independent contributions. The cannonball “CB2” dominates the radio AG at late times.

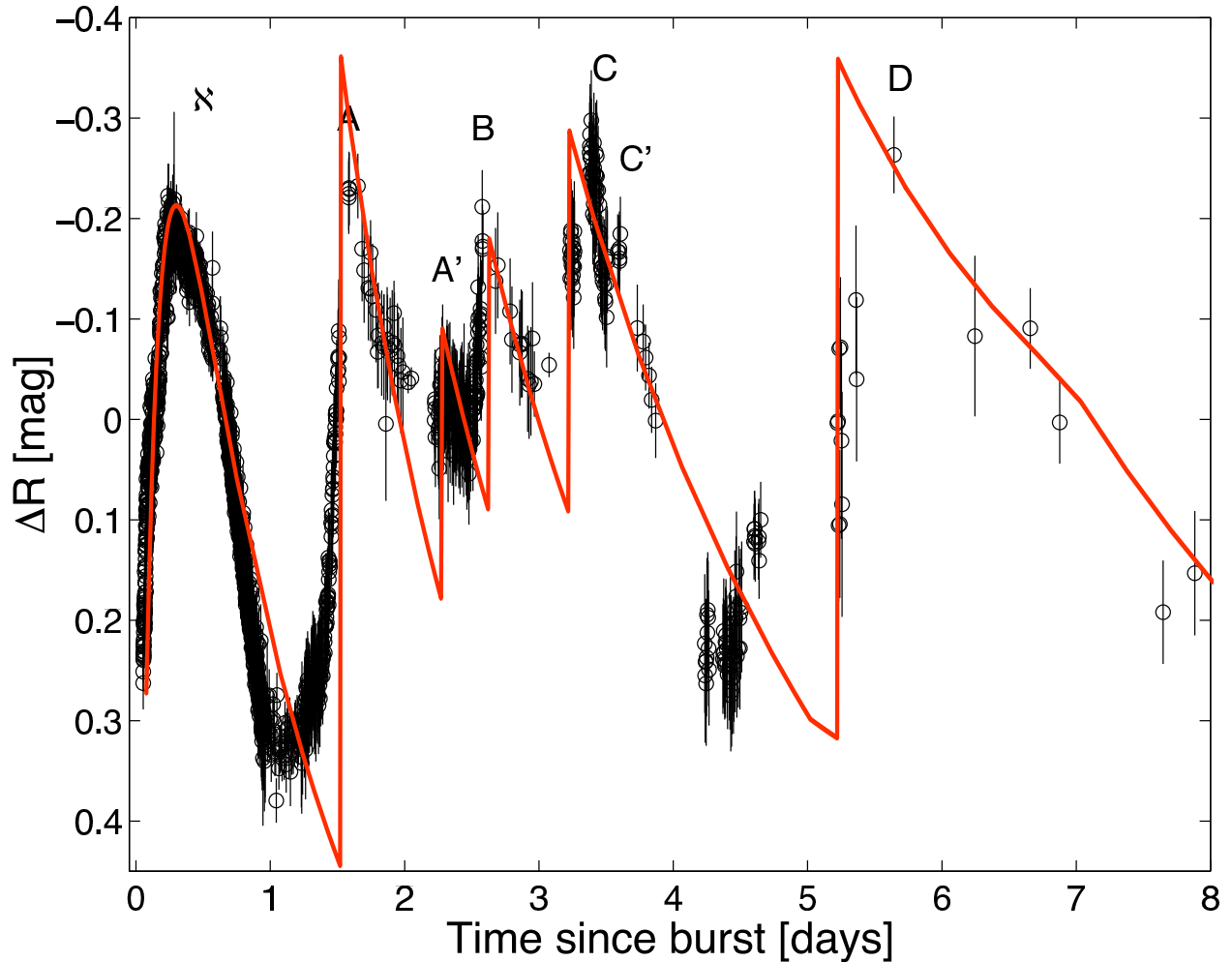


Fig. 7.— The R-band AG of GRB 030329, shown in two different ways. The “residua” ΔR of the data (the black points and circles) are the observed magnitudes relative to a broken power law of index $-\alpha$ jumping from ~ 1.1 to ~ 2 at $t \sim 5$ days (Lipkin et al. 2003). The (red) line represents the residua, relative to the same broken power law, of the “third round” CB-model fit described in the text. In the CB model, the \aleph feature is an artifact of comparing a smoothly-varying curve (the data or the CB-model fit for $t < 1$ day) to a power-law, which is theoretically unjustified at early times. The other features are real and have been modelled with the input density profile shown in Fig. (9).

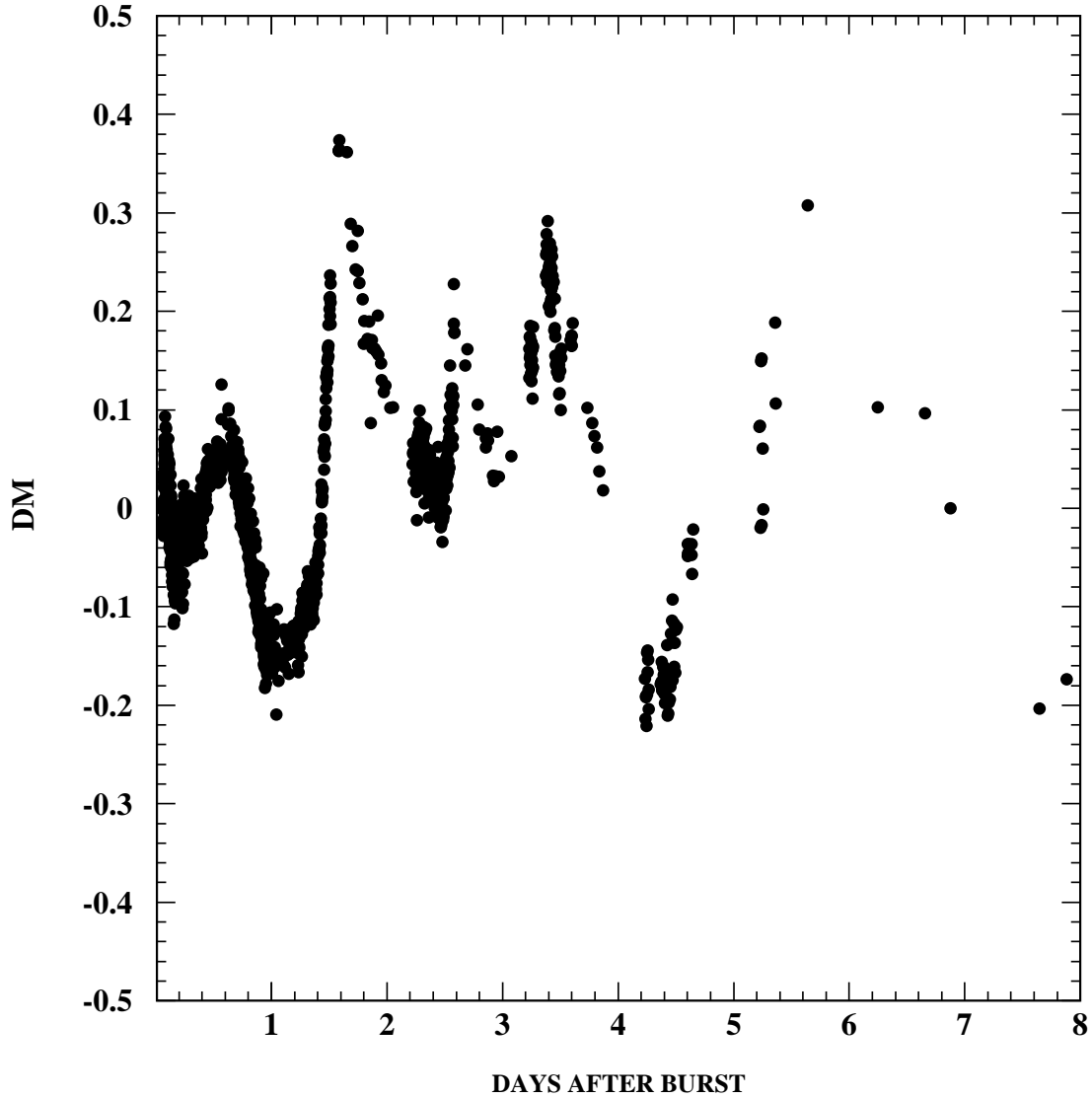


Fig. 8.— The magnitude-difference “residua” of the R-band AG data of GRB 030329 (shown here without error bars) relative to the “second-round” CB-model fit described in the text, for which the ISM density is assumed to be a constant plus a “wind” contribution declining as $1/r^2$. The prominent \aleph feature of Lipkin et al. (2003) is absent, while the features at $t > 1$ day are real.

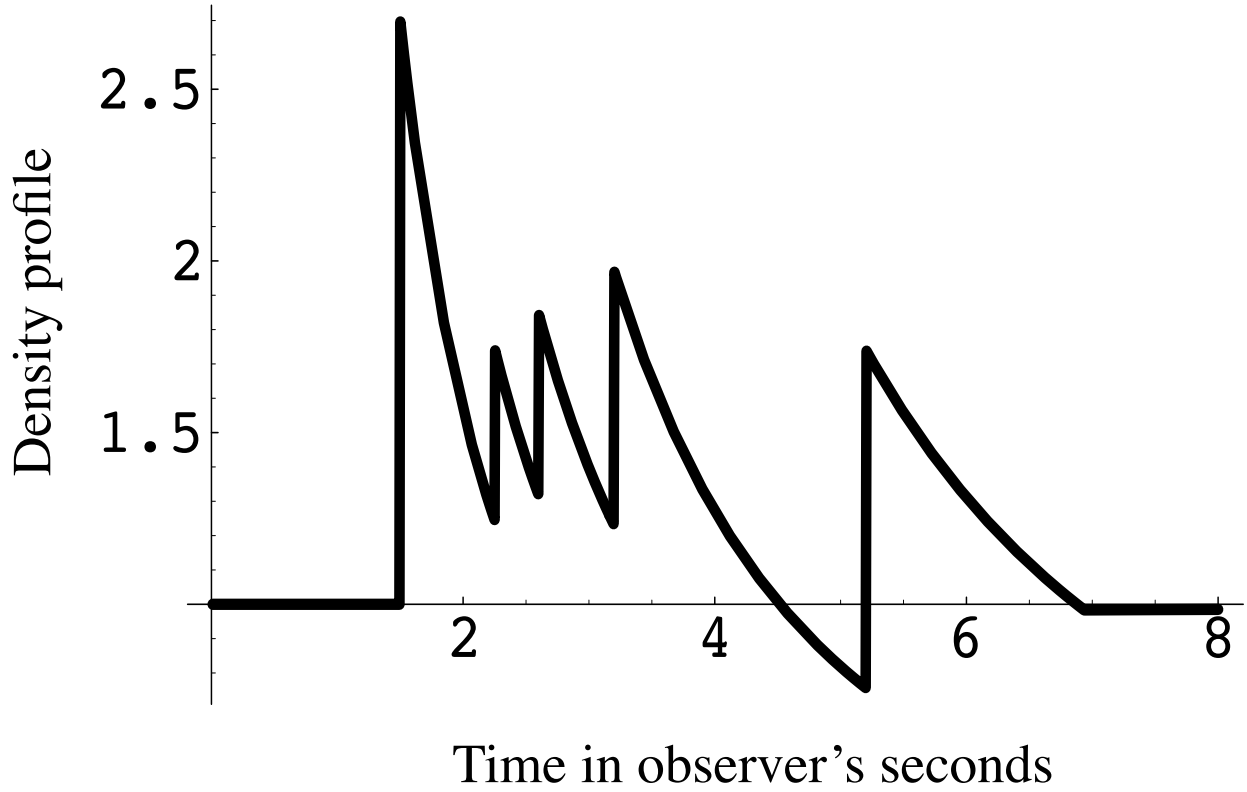


Fig. 9.— The “structured” density profile: the ISM density variations assumed in the “third round” CB-model fit to the R-band AG of GRB 030329 (relative to the smooth ISM density of the “second round” fit, assumed to be a constant plus a “wind” contribution decreasing as $1/r^2$).

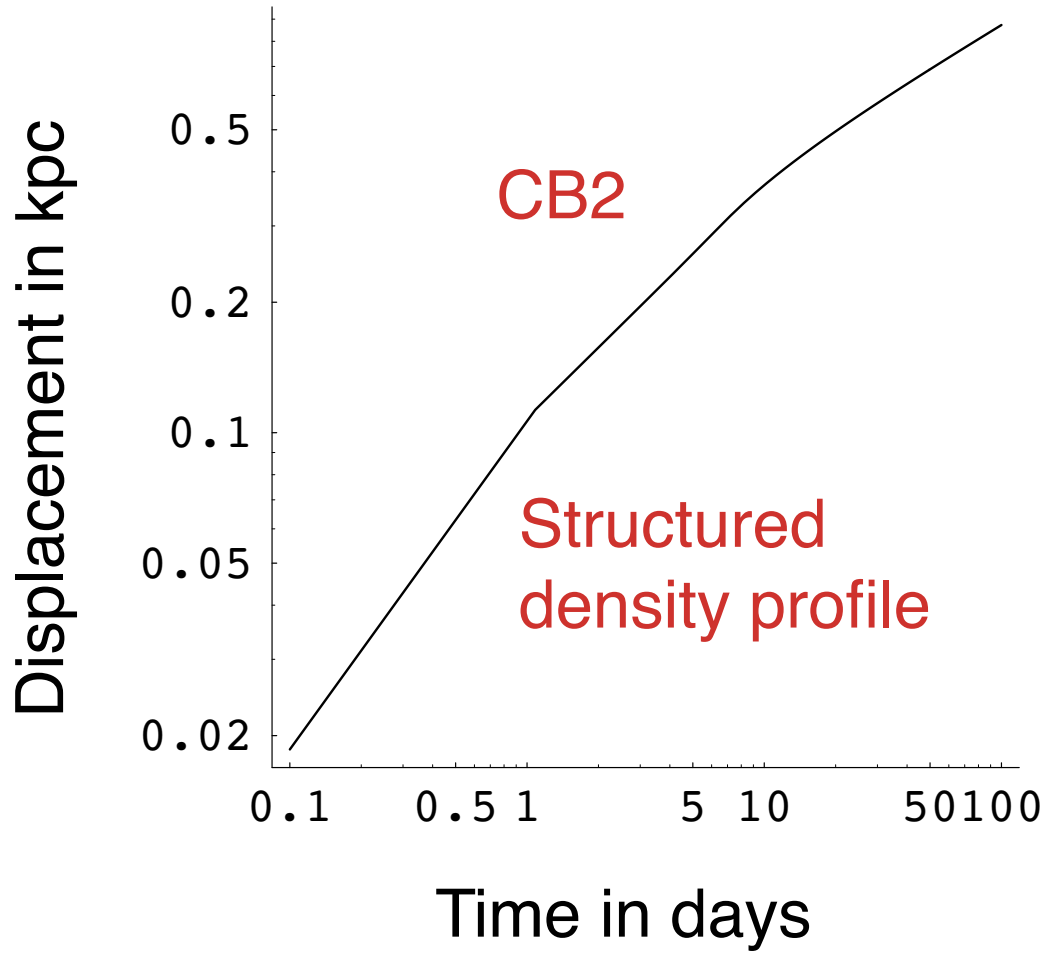


Fig. 10.— The distance in kpc, as a function of observer’s time, of the CB which dominates the AG of GRB 030329 at $t > 1.5$ days, and whose displacement in the sky is largest. The prediction is for the “third round” fit described in the text, with the structured density profile of Fig. (9), required to explain the features of the AG.

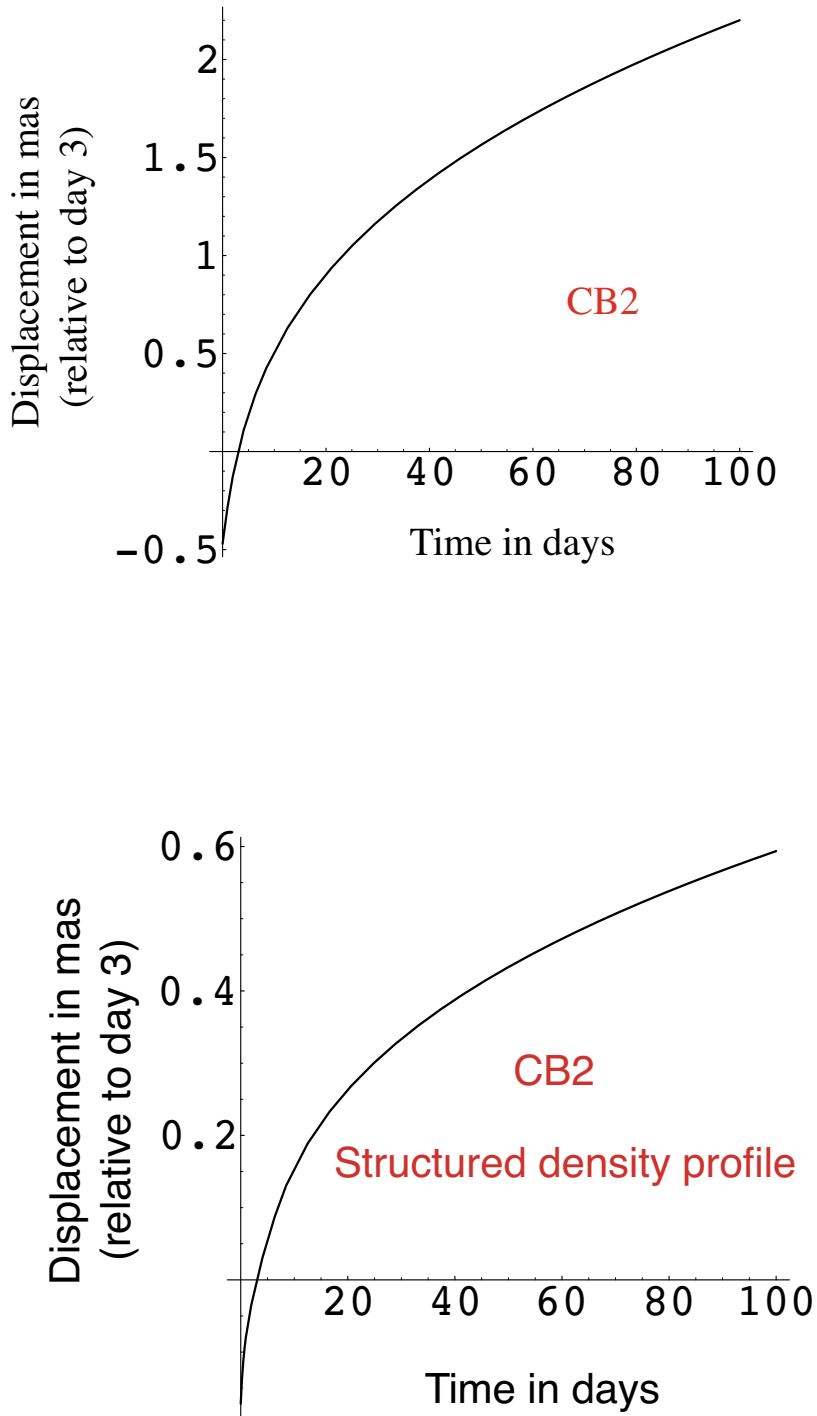


Fig. 11.— The predicted angular displacement in the sky (in mas) as a function of observer’s time, of the CB which dominates the AG of GRB 030329 at $t > 1.5$ days, and whose displacement is largest. The displacement is shown relative to the CB’s position at day 3. The upper panel is the prediction of Dar & De Rújula (2003b), wherein the effect of the observed “features” of the AG was ignored. The lower panel is the prediction for the “third round” CB-model fit described in the text, in which the cited effect is taken into account via the structured density profile of Fig. (9).